

JOINT INSTITUTE FOR NUCLEAR RESEARCH
Veksler and Baldin Laboratory of High Energy Physics

FINAL REPORT ON THE SUMMER STUDENT PROGRAM

Investigation of strongly interacting matter
produced at energies of beam energy scan
program at STAR

Supervisor: Alexey Aparin, JINR

Student: Betania Camille Tumelero Backes, Brazil
Federal University of Santa Catarina

Participation Period: July 07 - August 18

Dubna, 2018

Abstract

In this work we present a brief introduction to the Quantum Chromo-Dynamics and its phase diagram and try to identify one of the signatures of the phase transition between hadronic state of matter and the Quark Gluon Plasma (QGP) state, the enhanced strangeness production in heavy ion collisions, by calculating the K^+/π^+ ratio in heavy ion collisions using two different Monte Carlo generators. It is to be then compared to the results of Beam Energy Scan program results obtained at STAR detector at the Relativistic Heavy Ion Collider (RHIC).

Contents

| | | |
|----------|---|-----------|
| 1 | Introduction | 2 |
| 2 | Theory Overview | 3 |
| 3 | STAR Experiment | 4 |
| 4 | Models and methods | 4 |
| 4.1 | Therminator 2 | 4 |
| 4.2 | UrQMD | 5 |
| 5 | Therminator 2 Simulations and Results | 5 |
| 5.1 | p_T spectra for different particles | 6 |
| 5.2 | K^+/π^+ ratios | 6 |
| 5.3 | π^+/π^- and K^+/K^- ratios | 9 |
| 6 | UrQMD simulations and results | 10 |
| 6.1 | p_T spectra for different particles | 10 |
| 6.2 | K^+/π^+ ratios | 10 |
| 7 | Conclusions | 12 |
| 8 | Acknowledgements | 12 |

1 Introduction

Initially when Lee and Wick first proposed studying the high-energy nuclear collisions their goal was to create a new form of nuclear matter called the QGP [4]. It turns out that the net-baryon density as well as the temperature strongly depend on the colliding energy, therefore high-energy collisions are very effective for studying the QCD phase diagram. At mid-rapidity, the higher the collision energy the lower the net-baryon density. In ultra-relativistic heavy-ion collisions, where the net-baryon density is close to zero, the strongly coupled QGP has been observed at both RHIC and LHC. The properties of the medium created in such collisions show a strong opacity to colored objects and small ratio of shear viscosity over entropy density [5]. While the study of the nature of the sQGP continues in the high energy region, the first RHIC beam energy scan (RHIC BES1) program, has started in 2010. The main motivation there is to systematically explore the nuclear matter phase structure, the emergent property with the QCD degrees of freedom, at higher baryon density region.

Heavy ion collisions produce a big and diverse amount of particles at the final state of the collisions, producing events of great complexity. One of the most fundamental results of heavy ion collisions is the formation of the QGP, new phase state of nuclear matter with quark and gluon degrees of freedom. It has great impact on studies about nuclear processes that occur in the interior of stars and also on the comprehension of conditions in primordial states of the universe formation. In the search for the phase transition between the hadronic matter and the sQGP, a lot of different signatures can be investigated. In this work, we focus on the particle production of strange K^\pm and non-strange π^\pm in Au+Au collisions and in the ratios of this particle yields to try to identify characteristics of the QGP formation.

In the section 2, a brief theory introduction is given. In section 3, an overview of the STAR Experiment is presented. In section 4, a brief presentation about the tools used in the scope of this work is given. In sections 5 and 6, the results obtained are available. In section 7, the conclusions of this work are given.

2 Theory Overview

One of the major goals in high energy nuclear collisions is to determine the conditions behind the phase transition between hadronic matter (a state in which quarks and gluons are confined in composite particles, called baryons and mesons) and the QGP (a state of deconfined partonic matter). At high energies, Quantum Chromodynamics (QCD) predicts a phase transition, when hot and dense matter is melting, separating particles into a plasma where colored partons (quarks and gluons) became quasi-free and no longer confined into colorless doublets (mesons) and triplets (barions).

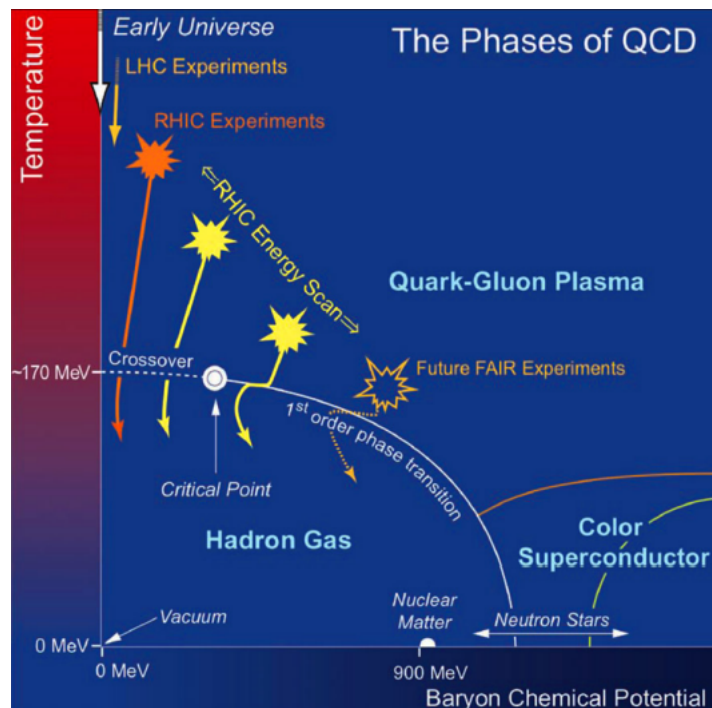


Figure 1: Conjectured version of the QCD phase diagram with μ_B on the horizontal axis and Temperature (in energy units) on vertical axis. Figure extracted from [7].

The most accessible way of experimentally characterizing the phase diagram is in the plane of temperature (T) and baryon chemical potential (μ_B), as shown in Figure 1. For values close to $\mu_B = 0$, experiments at the Large Hadron Collider (LHC) and the Relativistic Heavy Ion Collider (RHIC) have provided evidence of the QGP formation, but exact parameters of the first order phase transition location and existence of the critical point at higher μ_B is yet to be confirmed experimentally.

There are several methods used in the search for the critical point and for the first order phase transition at energies of BES, related to different experimental characteristics of the QGP formation. Some different approaches used in attempts to study the first order phase transition and the critical point can be found in [7].

In this work, the ratios between K/π produced in the gold-gold collisions were used as a signature of phase transition of interest. Enhanced production of strangeness has been predicted as a prominent signature of the QGP formation [1]. As a reference, the formation of the Quark Gluon Plasma is unlikely in elementary pp collisions, so that enhanced strangeness production in heavy ion collisions in comparison to pp could be a sign of QGP formation. Even though it is not a sufficient signature, the presence of enhanced strangeness production is a necessary condition for the QGP formation.

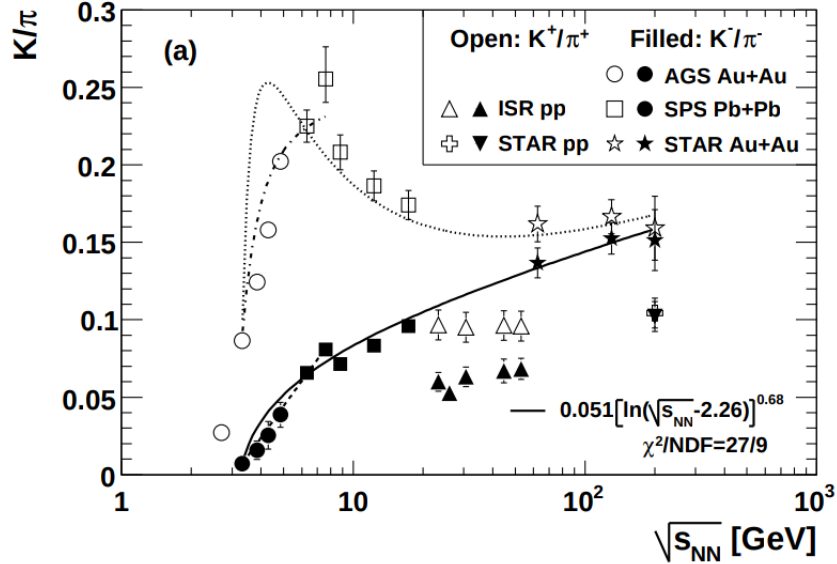


Figure 2: Figure extracted from [1]. Experimental data from the K/π ratio in central heavy ion collisions and in pp collisions. It shows a peak in the K^+/π^+ production, referred to as "the horn".

Figure 2, extracted from [1], shows experimental data from K/π ratios, where it can be seen that while K^-/π^- increases with $\sqrt{s_{NN}}$, K^+/π^+ has a peak around 10 GeV, referred to as the "horn", which doesn't seem to be explained by ordinary physics, being attributed to a phase transition between hadronic matter and QGP.

The main goal of this work is to reproduce this effect with two different event generators (UrQMD and THERMINATOR 2), watching the differences between the results and comparing it to experimental data.

3 STAR Experiment

A Solenoidal Tracker At RHIC (STAR) is one of two currently operational detectors on RHIC collider. It was originally designed to detect heavy ion collision (mainly gold-gold) at maximal energies of $\sqrt{s_{NN}} = 200$ GeV. It is capable of detecting over a thousand charged particles in the most central collisions of heavy ions. The main detector of the STAR experiment is the Time Projection Chamber (TPC). The cylindrical axis of the TPC is aligned to the beam direction and is referred to as the z-direction. The TPC provides the full azimuthal coverage ($0 \leq \phi \leq 2\pi$) and a pseudorapidity. The STAR detector system is shown in Figure 3.

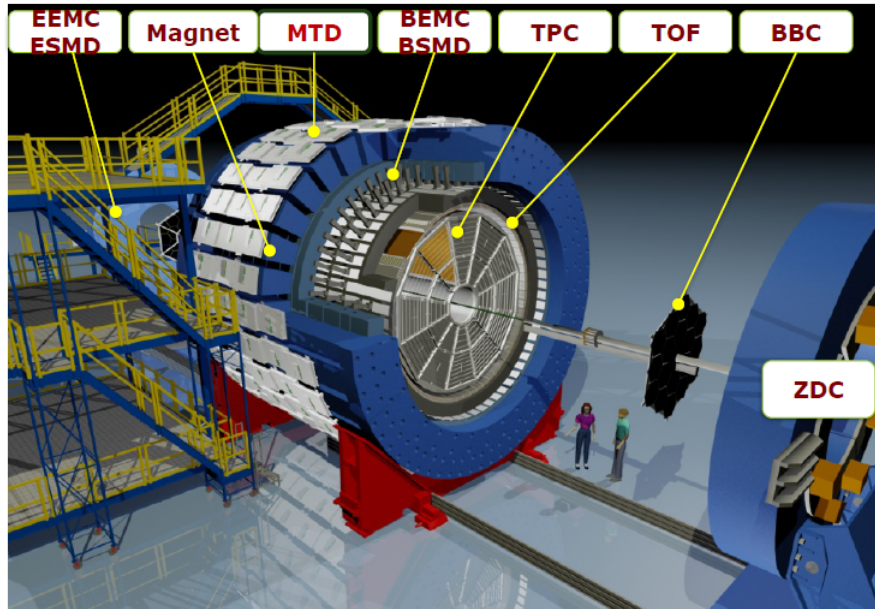
Figure 4, extracted from [6] shows the experimental p_T spectra for the particles of interest in the scope of this work for various centrality classes.

4 Models and methods

4.1 Therminator 2

In the context of heavy-ion collisions, the statistical approach has proved to be really useful for a wide range of observables. In order to generate statistics and calculate the K^+/π^+ and K^-/π^- ratios in Au+Au collisions THERMINATOR 2 [2], the THERMal heavy IoN generATOR 2, was used. It consists of a Monte Carlo event generator dedicated to statistical production of particles in heavy-ion collisions. It is written in C++ and uses the CERN ROOT environment. The program has some different freeze-out models that can be chosen, and with few input parameters, such as temperature, chemical potentials and the energy in the center-of-mass frame ($\sqrt{s_{NN}}$), the output ROOT file is generated. In the output file, the statistics for mass, space-time coordinates, energy and momentum coordinates, decay flag, PDG identification number, parent

STAR Detector System



9

Figure 3: The STAR detector system.

PDG number, root particle PDG number, sequence number in the event, parent sequence number of the event and the event id are given for each event and particle created in the collision. With those outputs, experimental data analysis, detector modeling and estimates for heavy-ion collisions at RHIC, LHC, SPS, FAIR or NICA can be done¹.

4.2 UrQMD

The Ultra Relativistic Quantum Molecular Dynamics² (UrQMD) model is a transport model for simulating heavy-ion collisions. It was used to generate statistics for AuAu collisions so that the ratios of K^+/π^+ and K^-/π^- could be calculated and compared to the results obtained with THERMINATOR 2. To run this program, the energy in the center-of-mass frame ($\sqrt{s_{NN}}$), the number of events and the freeze-out time are given as inputs for AuAu collisions, which is simpler than what is fed to the previous generator, that uses chemical potentials and temperature as input parameters. The outputs given by UrQMD are similar to the ones given by THERMINATOR 2, so that it is easy to compare the results given between the two generators. It is important to say that UrQMD model doesn't have a phase transition mechanism, therefore the results expected with this model and from THERMINATOR 2 are different.

5 Therminator 2 Simulations and Results

Following what was introduced in Section 4.1, for the THERMINATOR 2 calculations, the freeze-out model used for was Lhyquid 2+1D Boost-Invariant Hydro, which needs the temperature, the beam energy ($\sqrt{s_{NN}}$) and the baryonic chemical potential (μ_B). The numerical values of those parameters were taken from experimental data [3] for the energies of $\sqrt{s} = 2.24, 2.32, 4.86, 6.27, 7.62, 8.77, 12.3$ and 17.3 GeV. These energies are consistent with experimental ones from BES-I and planned BES-II. Using the program, fifty

¹For further information, the reader is referred to the original paper [2].

²User guide and download information and more deep information about the program are available at <https://urqmd.org/>.

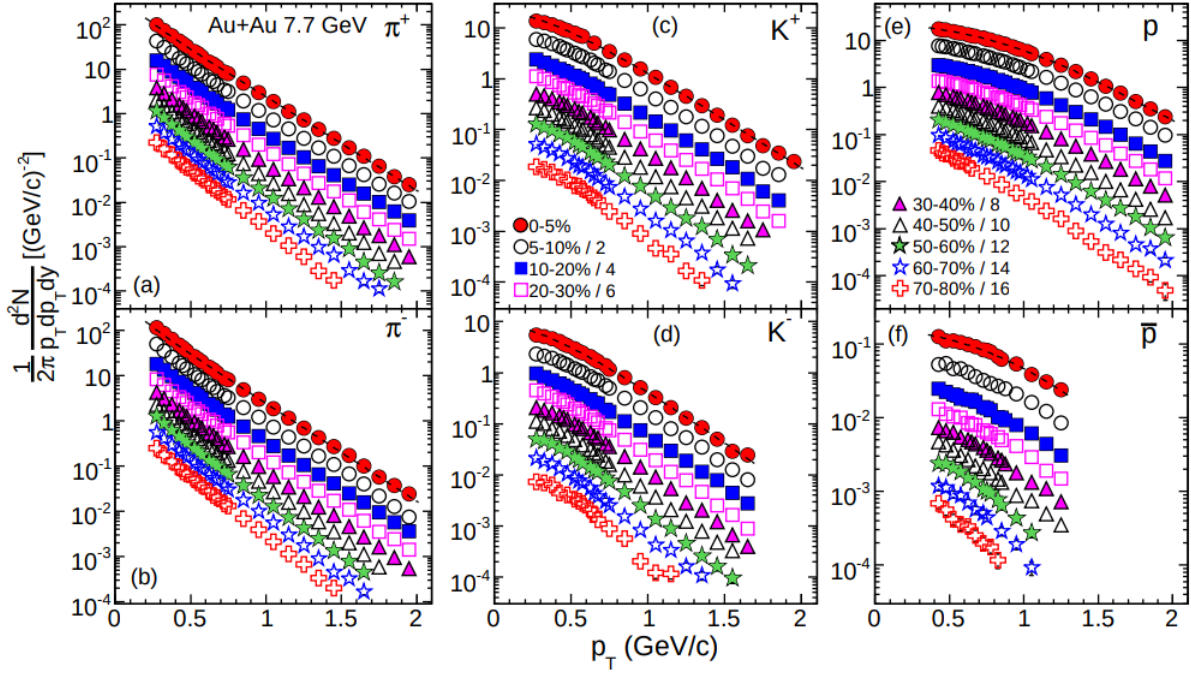


Figure 4: Figure and caption extracted from [6]. (Color online) Mid-rapidity ($|y| < 0.1$) transverse momentum spectra for (a) π^+ , (b) π^- , (c) K^+ , (d) K^- , (e) p , and (f) \bar{p} in Au+Au collisions at $\sqrt{s_{NN}} = 7.7$ GeV for different centralities. The spectra for centralities other than 0–5% are scaled for clarity as shown in figure. The curves represent the Bose-Einstein, m_T -exponential, and double-exponential function fits to 0–5% central data for pions, kaons, and (anti-) protons, respectively. The uncertainties are statistical and systematic added in quadrature.

thousand events were generated for each energy in order to do the calculations of interest in this project, being those the energies of interest in the region on which the “horn” effect should appear.

5.1 p_T spectra for different particles

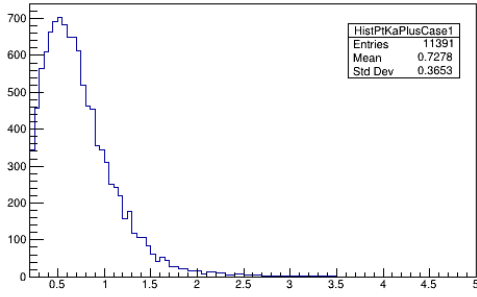
The spectra for transverse momentum are presented in Figures 5 and 6. They were made by reading all the root tree files with the generated events with THERMINATOR 2, reading the branches with the information about momentum coordinates p_x and p_y to calculate transverse momentum $p_T = \sqrt{p_x^2 + p_y^2}$ and then calculate the pseudorapidity $\eta = \sinh^{-1}(p_z/p_T)$ to make the cut-offs. There are two separated groups of histograms: (i) Only for particles with $\eta \leq 1.0$; (ii) Only for particles with $\eta \leq 0.5$. The results are shown separately for K^\pm and for π^\pm .

5.2 K^+/π^+ ratios

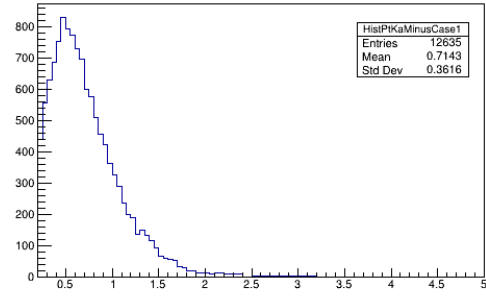
The K^+/π^+ ratio was calculated for all the energies in which statistics were generated. The result can be seen in Figure 7.

The initial conditions fed to the generator were the temperature and the baryon chemical potential, both extracted from [3]. It can be seen that both K^+/π^+ and K^-/π^- ratios increase steadily with $\sqrt{s_{NN}}$, which is not consistent with experimental observations, since the peak that characterizes the “horn” does not appear as shown previously in Figure 2.

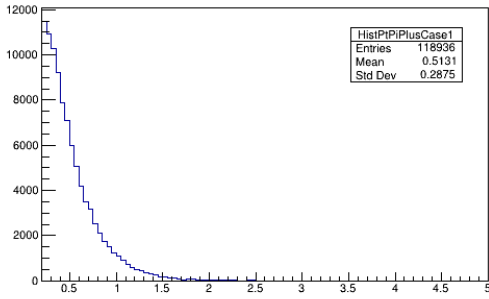
This result was then modified by applying minimal cut conditions by selecting only the particles with $\eta \leq 1.0$ and $p_T \geq 0.2$, which changed numerical results but not the trend or steady growth. That could be related to the cuts not being enough or to the initial conditions that were changed due to lack of experimental



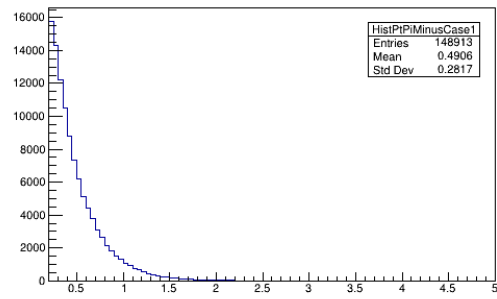
(a) K^+ with $|\eta| \leq 1.0$



(b) K^- with $|\eta| \leq 1.0$

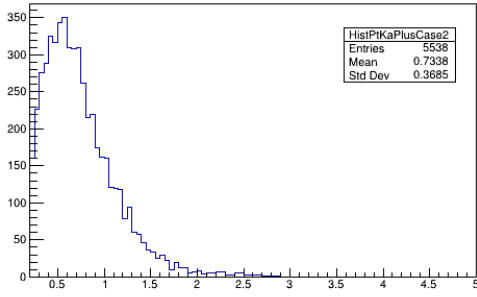


(c) π^+ with $|\eta| \leq 1.0$

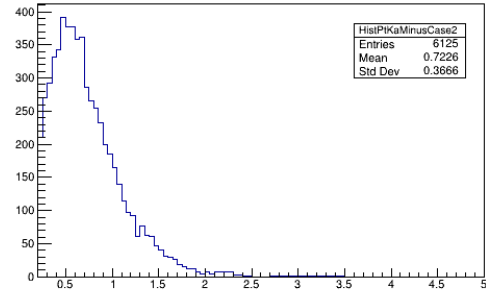


(d) π^- with $|\eta| \leq 1.0$

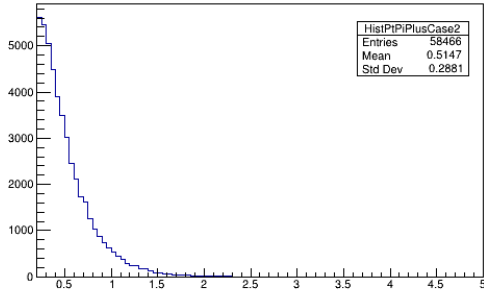
Figure 5: Histograms of transverse-momentum for the energy $\sqrt{s_{NN}} = 7.62$ GeV with cut of pseudorapidity $|\eta| \leq 1.0$ and $p_T \geq 0.2$ for different particles generated with THERMINATOR 2.



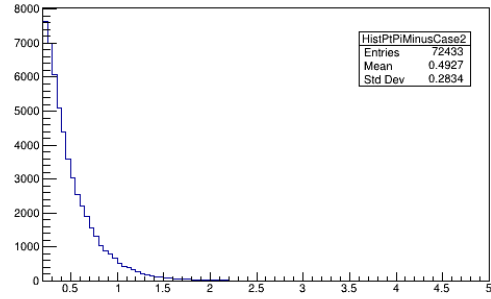
(a) K^+ with $|\eta| \leq 0.5$



(b) K^- with $|\eta| \leq 0.5$



(c) π^+ with $|\eta| \leq 0.5$



(d) π^- with $|\eta| \leq 0.5$

Figure 6: Histograms of transverse-momentum for the energy $\sqrt{s_{NN}} = 7.62$ GeV with cut of pseudorapidity $|\eta| \leq 0.5$ and $p_T \geq 0.2$ for different particles generated with THERMINATOR 2.

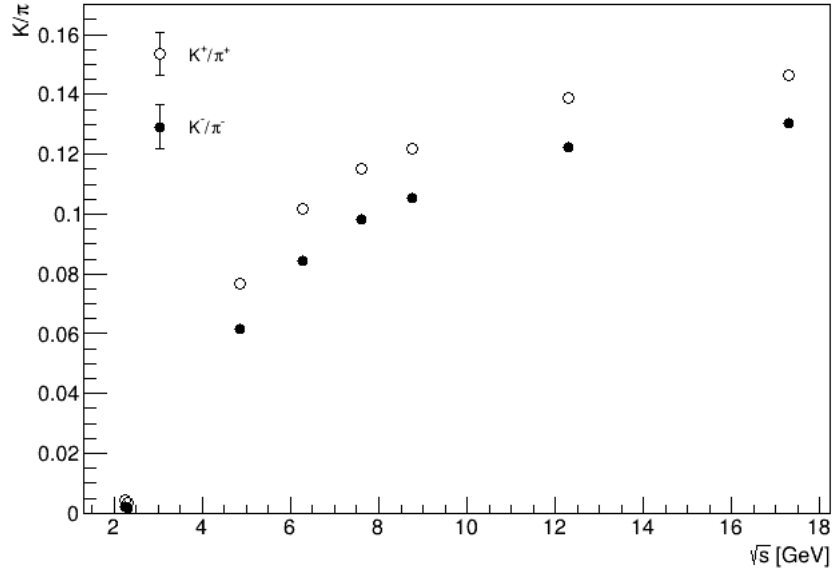


Figure 7: Results obtained with Therminator 2 for the K/π ratio.

data. If those conditions, such as strangeness potential (μ_S), occur to fluctuate significantly with the beam energy it could justify the results obtained.

5.3 π^+/π^- and K^+/K^- ratios

In order to investigate what was causing the behavior of the K/π ratio, the π^+/π^- and K^+/K^- ratios were calculated. From experimental data, it is known that for low energies, the strange particles ratio K^+/K^- have high values at very low energies and decrease with energy growth[1]. The expected result, extracted from [1] is shown in Figure 8, while the results for both K^+/K^- and π^+/π^- obtained with THERMINATOR 2 statistics are shown in Figure 9.

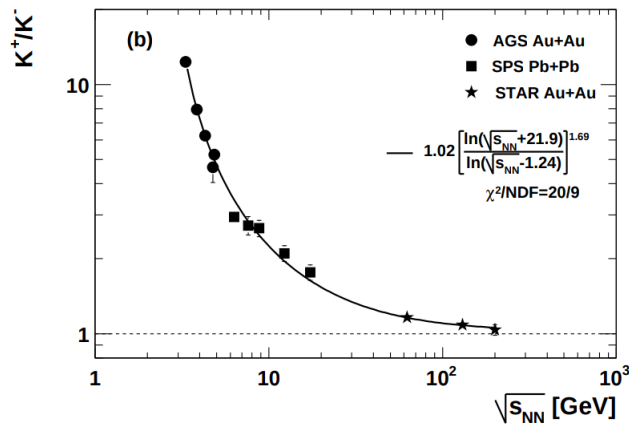


Figure 8: Figure extracted from [1]. Here the experimental data for K^+/K^- ratio is shown.

A fit was made to see if the result followed the same behavior as the experimental data, using the same

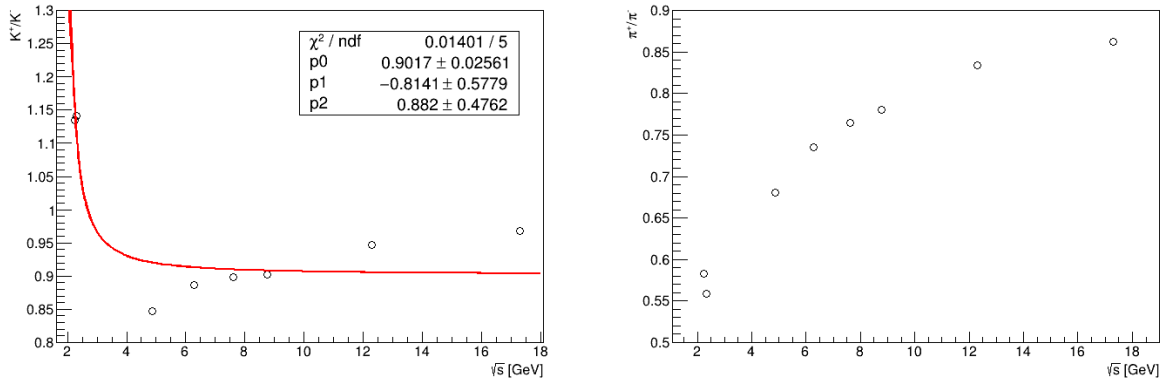


Figure 9: Results obtained with Therminator 2 for the K^+/K^- ratio (left) and for the π^+/π^- ratio (right).

curve as in [1] with three free parameters. The final fit result for the fit line in Figure ?? is eq. 1

$$0.9017 \left[\frac{\ln(\sqrt{s_{NN}} - 0.8141)}{\ln(\sqrt{s_{NN}} + 0.882)} \right]^{1.69} \quad (1)$$

Comparing Figures 8 and 9, what can be concluded is that the number of K^+ is being extremely underestimated in comparison to experimental observations, what could justify why the expected behavior for K^+/π^+ was not observed when no cuts are being made.

6 UrQMD simulations and results

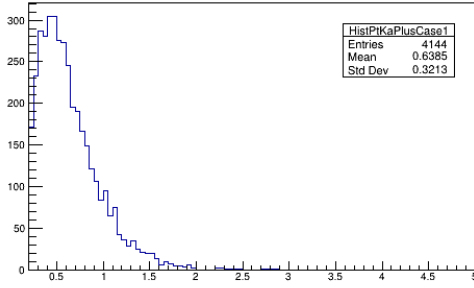
Following what was exposed in section 4.2, statistics were generated for the energies of $\sqrt{s_{NN}} = 7.7$ and 11.5 GeV as an attempt to reproduce the “horn”. For each energy, fifty thousand events were generated in UrQMD. The output files used in this work were the f14 files, that were converted into ROOT tree files for a better analysis of the generated events.

6.1 p_T spectra for different particles

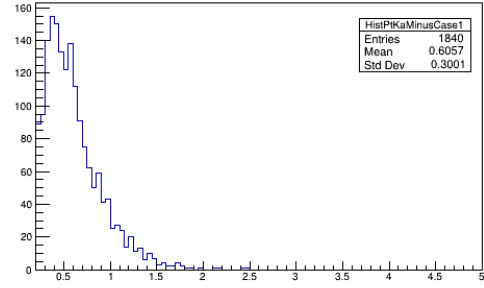
The p_T spectra for transverse momentum are presented in Figures 10 and 11. They were made by generating ROOT tree files from f14 output file from UrQMD and making a similar analysis to the one made with the ROOT tree files generated automatically with THERMINATOR 2. The transverse momentum and the pseudorapidity were calculated and used as a way to select only the particles of interest. The results are shown separately for K^\pm and π^\pm . Only the particles with $p_T \geq 0.2$ were selected, and they were separated into the ones with $|\eta| \leq 1.0$ and the ones with $|\eta| \leq 0.5$.

6.2 K^+/π^+ ratios

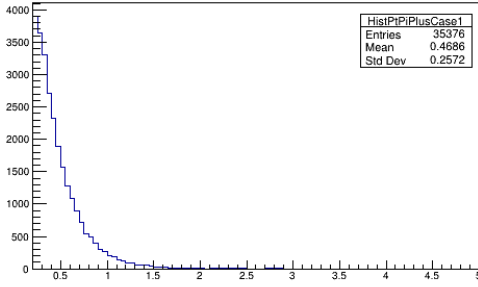
The K/π ratio was calculated with the statistics generated with UrQMD. Without any cuts, the result was similar to the one obtained with THERMINATOR 2, with both of them raising with $\sqrt{s_{NN}}$. However, when just the particles with $p_T \geq 0.2$ and $|\eta| \leq 1.0$ were selected, the obtained result was closer to the experimental data from [1], being lower for the K^-/π^- ratio and probably having a peak. The exact location of the peak could not be determined, since there was not enough time for generating statistics for a large amount of energies, remaining as a further work yet to be done. Further analysis selecting only the most central collisions can be done in the search for improving the results.



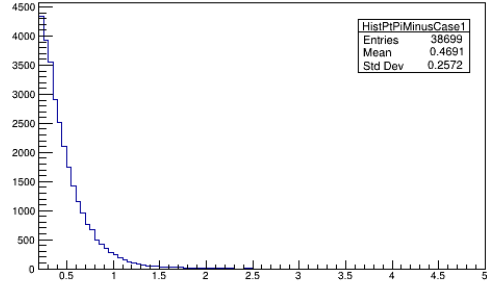
(a) K^+ with $|\eta| \leq 1.0$



(b) K with $|\eta| \leq 1.0$

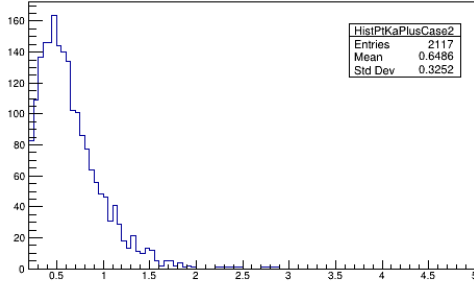


(c) π^+ with $|\eta| \leq 1.0$

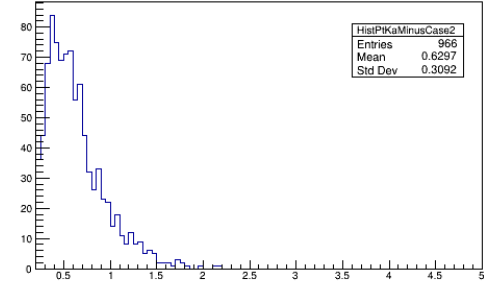


(d) π^- with $|\eta| \leq 1.0$

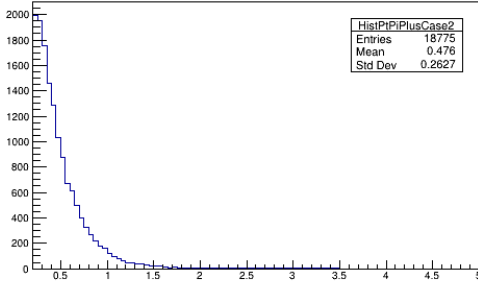
Figure 10: Histograms of transverse-momentum for the energy $\sqrt{s_{NN}} = 7.7$ GeV with cut of pseudorapidity $|\eta| \leq 1.0$ and $p_T \geq 0.2$ for different particles generated with UrQMD.



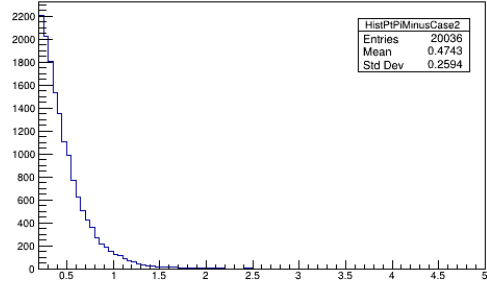
(a) K^+ with $|\eta| \leq 0.5$



(b) K with $|\eta| \leq 0.5$



(c) π^+ with $|\eta| \leq 0.5$



(d) π^- with $|\eta| \leq 0.5$

Figure 11: Histograms of transverse-momentum for the energy $\sqrt{s_{NN}} = 7.62$ GeV with cut of pseudorapidity $|\eta| \leq 0.5$ and $p_T \geq 0.2$ for different particles generated with UrQMD.

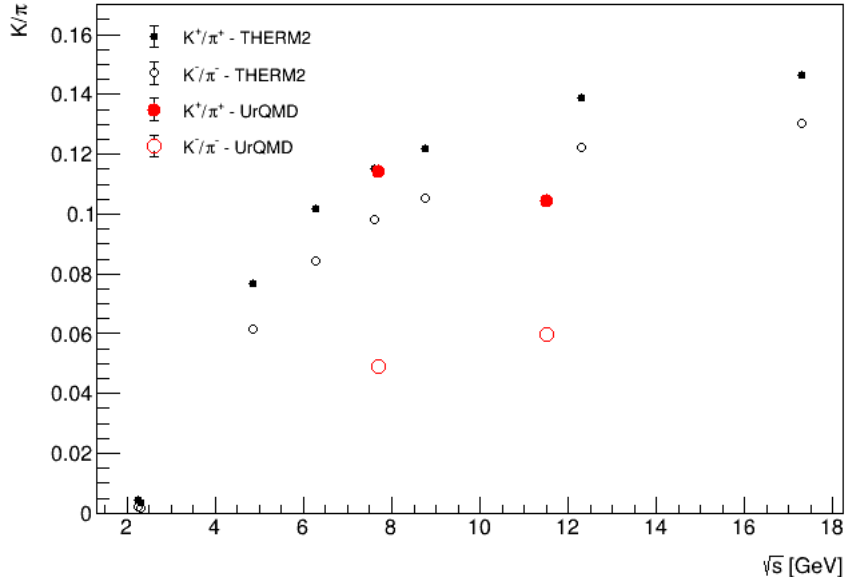


Figure 12: K/π ratios calculated with both THERMINATOR 2 and UrQMD.

7 Conclusions

The final results with THERMINATOR 2 were not in agreement with experimental data when minimal cuts were made, selecting only the particles with $|\eta| \leq 1.0$ and $p_T \geq 0.2$ or when no cuts were made. The number of K^+ is underestimated when compared to the number of experimentally produced kaons. One of the possible reasons for having that effect is that the strangeness potential was kept the same for all energies while running THERMINATOR 2, and if it is dependent on the center of mass energy, $\sqrt{s_{NN}}$, the obtained result might have been different. Another possible source of error might be not making enough cuts. Further investigation on selecting only the most central collisions can be done to try to reproduce the “horn” effect with the THERMINATOR 2 statistics, since making a better selection of the events could make the expected behavior appear.

The final results with UrQMD have shown that the presence of a peak is observable around the energies on which it occurs experimentally when only the particles with $|\eta| \leq 1.0$ and $p_T \geq 0.2$ are selected. To make a further and deeper analysis, more statistics should be generated with UrQMD for different values of the energy in the center of mass frame. Besides that, other cuts can be made, selecting only the most central collisions.

8 Acknowledgements

I would like to express my profound gratitude to my supervisor Alexey Aparin for the opportunity and for the support throughout the course of this project. I express my gratitude to Debora Peres Menezes, my supervisor in Brazil, who encouraged me to apply on this program and who always supported me. Lastly, I would like to thank the Organizing Committee of the Summer Student Program for the amazing opportunity of being part of this experience and for financial support.

References

- [1] B. Abelev et al., “Systematic Measurements of Identified Particle Spectra in pp, d+Au and Au+Au Collisions from STAR,” Phys. Rev., vol. C79, p. 034909, 2009.

- [2] M. Chojnacki, A. Kisiel, W. Florkowski, and W. Broniowski, “THERMINATOR 2: THERMal heavyIoN generATOR 2,” 2011.
- [3] J. Cleymans, H. Oeschler, K. Redlich, and S. Wheaton, “Comparison of Chemical Freeze-Out Criteria in Heavy-Ion Collisions,” *Phys. Rev.*, vol. C73, p. 034905, 2005.
- [4] T.D. Lee and G.C. Wick, *Phys. Rev.* D9, 2291(1974).
- [5] M. Gyulassy and L. McLerran, *Nucl. Phys.* A750, 30(2005).
- [6] STAR Collaboration: L. Adamczyk et al., “Bulk Properties of the Medium Produced in Relativistic Heavy-Ion Collisions from the Beam Energy Scan Program”, 2017
- [7] STAR Collaboration, “Studying the Phase Diagram of QCD Matter at RHIC”, 2014
<https://drupal.star.bnl.gov/STAR/starnotes/public/sn0598>
- [8] <https://urqmd.org/>